ARTICLE
Journal of Cellular Biochemistry 112:1450–1457 (2011)

Journal of Cellular Biochemistry

# Effect of β-Amyloid (25–35) on Mitochondrial Function and Expression of Mitochondrial Permeability Transition Pore Proteins in Rat Hippocampal Neurons

Rui Ren,[1] Yang Zhang,[1] Benchang Li,[2] Yanping Wu,[1] and Baixiang Li[1*]

[1]*Toxicology Group, Public Health College, Harbin Medical University, Harbin, PR China*

[2]*Toxicology Group, Institute of Occupational Disease Prevention, Nanchang, Jiangxi Province, PR China*

## ABSTRACT

The aim of this study was to assess the effect of the β-amyloid fragment $A\beta_{25-35}$ on mitochondrial structure and function and on the expression of proteins associated with the mitochondrial permeability transition pore (MPTP) in rat hippocampal neurons. Ninety clean-grade Sprague–Dawley rats were randomly assigned to six groups (n = 15 per group). $A\beta_{25-35}$ (1, 5, or 10 μg/rat) was injected into hippocampal area CA1. Normal saline was injected as a control. The effect of $A\beta_{25-35}$ injection on hippocampal structure was assessed by transmission electron microscopy. $Ca^{2+}$-ATPase activity, $[Ca^{2+}]_i$, and mitochondrial membrane potential were measured. The expression of genes associated with the MPTP, including the voltage-dependent anion channel (VDAC), adenine nucleotide translocator (ANT), and cyclophilin D (Cyp-D), were evaluated. Results showed that $A\beta_{25-35}$ injection damaged the mitochondrial structure of hippocampal neurons, decreased $Ca^{2+}$-ATPase activity and mitochondrial membrane potential, and increased $[Ca^{2+}]_i$. The expression levels for VDAC, ANT, and Cyp-D in all groups were significantly ($P < 0.05$) higher than those in the normal control group after $A\beta_{25-35}$ injection. These results indicate that $A\beta_{25-35}$ damages mitochondria in rat hippocampal neurons and effects mitochondrial dysfunction, as well as increasing the expression of genes associated with the MPTP. Mitochondrial dysfunction may result in increased *MPTP* gene expression, leading to neurodegenerative effects. J. Cell. Biochem. 112: 1450–1457, 2011. 

**KEY WORDS:** β-AMYLOID; MITOCHONDRIA; MITOCHONDRIAL PERMEABILITY TRANSITION PORE

β-Amyloid (Aβ) is the major component of senile plaques, histopathologic alterations observed in diseases such as Alzheimer disease. Excessive expression, aggregation, and deposition of Aβ, particularly the $A\beta_{25-35}$ fragment, in the brain are considered to underlie certain neurodegenerative diseases [Millucci et al., 2010]. Mitochondria comprise the main center for energy transfer between intracellular and extracellular compartments and play important roles in the maintenance of cell function and in apoptosis. Increasing evidence supports the concept of mitochondrial dysfunction in neurodegenerative diseases [Burchell et al., 2010]. Studies have shown that Aβ can cause damage to mitochondrial structure and function [Casley et al., 2002; Reddy, 2009; Manczak et al., 2010] and lead to apoptosis [Ferreiro et al., 2008]. Direct deposition of Aβ in the mitochondria [Chen and Yan, 2007], and the involvement of nicotinamide adenine dinucleotide phosphate oxidase [Abramov et al., 2004], phospholipase $A_2$ [Zhu et al., 2006], and the mitochondrial permeability transition pore (MPTP) [Du and Yan, 2010; Muirhead et al., 2010], have been reported, but the specific mechanism underlying the effect of Aβ on mitochondria and in relation to neurodegenerative disease remains unclear.

The $A\beta_{25-35}$ fragment has also been shown to decrease ATPase activity in neurons [Mark et al., 1995]. Mitochondrial function is heavily affected by and involved in intracellular calcium signaling; mitochondrial $Ca^{2+}$ concentration increases with increased cytosolic $Ca^{2+}$. Mitochondrial $Ca^{2+}$ transport affects the activities of $Ca^{2+}$-sensitive metabolic enzymes in the mitochondrial matrix and regulates mitochondrial metabolism and also regulates intracellular $Ca^{2+}$ concentration ($[Ca^{2+}]_i$) via uptake or release of $Ca^{2+}$ [Celsi et al., 2009]. It has been reported that increased

Abbreviations Used: ANT, adenine nucleotide translocator; Cyp-D, cyclophilin D; DMSO, dimethylsulfoxide; MPTP, mitochondrial permeability transition pore; RT-PCR, reverse-transcription polymerase chain reaction; VDAC, voltage-dependent anion channel

Grant sponsor: Chinese National Natural Science Foundation; Grant number: 30600504.

*Correspondence to: Baixiang Li, PhD, Toxicology Group, Public Health College, Harbin Medical University, #157 Baojian Road, Harbin, Helongjiang Province 150081, PR China. E-mail: libaixianghmu@yahoo.com.cn

Received 24 August 2010; Accepted 28 January 2011 • DOI 10.1002/jcb.23062 • © 2011 Wiley-Liss, Inc.

Published online 14 February 2011 in Wiley Online Library (wileyonlinelibrary.com).

mitochondrial $Ca^{2+}$ results in opening of the MPTP [Baumgartner et al., 2009].

The MPTP is a composite channel spanning the inner and outer mitochondrial membranes and plays a critical role in maintaining mitochondrial function. Although the properties of the MPTP are well characterized, its exact molecular makeup remains a matter of debate [Halestrap, 2009; Zorov et al., 2009]. Associated proteins include the voltage-dependent anion channel (VDAC), located in the outer mitochondrial membrane, and the adenine nucleotide translocator (ANT), located in the inner mitochondrial membrane, as well as hexokinase II in the cytoplasm, creatine kinase between the inner and outer mitochondrial membranes, cyclophilin D (Cyp-D) in the mitochondrial matrix, Bcl-2/Bax in the outer mitochondrial membrane, and the peripheral benzodiazepine receptor. Under normal physiologic conditions, the MPTP has a low permeability and opens reversibly. However, under pathologic conditions, the MPTP is in an open state with high permeability, resulting in mitochondrial swelling, decreased mitochondrial membrane potential, and release of cytochrome *c*, Smac, and other proteins such as apoptosis-inducing factor, eventually leading to cell damage, apoptosis, or necrosis [Halestrap et al., 2004].

Given that mitochondrial dysfunction is involved in neurodegenerative diseases, the MPTP has become a target for the development of pharmacologic and perhaps molecular treatments [Galiegue et al., 2003; Kroemer, 2003; Emerit et al., 2004]. Thus, it is important to elucidate molecular mechanisms influencing mitochondrial membrane permeability. We hypothesized that Aβ affects mitochondrial function in neurons by regulating $Ca^{2+}$-ATPase, $[Ca^{2+}]_i$, and the expression of genes associated with the MPTP. The aim of the present study was to assess β-amyloid fragment $A\beta_{25-35}$-induced mitochondrial structural damage as well as its effects on mitochondrial function and *MPTP* gene expression in rat hippocampal neurons.

## MATERIALS AND METHODS

### MATERIALS

Ninety clean-grade adult Sprague Dawley rats (200–250 g; 45 male, 45 female) were purchased from Shanghai Slack Experimental Animal Center. The rats were housed according to the National Institutes of Health *Care and Treatment of Laboratory Animals*. The study protocol was approved by the Ethics Committee of Harbin Medical University (Harbin, China).

The amyloid $A\beta_{25-35}$ fragment was purchased from Sigma–Aldrich (St. Louis, MO); a total RNA extraction kit (Trizol) was purchased from Invitrogen (Carlsbad, CA); reverse-transcription (RT) and RT polymerase chain reaction (PCR) kits were purchased from Promega Corp. (Madison, WI); DNA markers were purchased from Fermentas Int. (Burlington, Canada); Fluo-3/AM was purchased from Invitrogen; Rhodamine 123 was purchased from Sigma–Aldrich; a $Ca^{2+}$-ATPase kit was purchased from Nanjing Jiancheng Biotechnology Co. (Nanjing, China); ANT goat polyclonal antibody, VDAC1 goat polyclonal antibody, and β-actin rabbit polyclonal antibody were purchased from Santa Cruz Biotechnology (Santa Cruz, CA); Cyp-D rabbit polyclonal antibody was purchased from Abcam (Cambridge, MA); alkaline phosphatase-conjugated anti-rabbit secondary antibody was purchased from Promega Corp.; and alkaline phosphatase-conjugated anti-goat secondary antibody was purchased from Santa Cruz Biotechnology.

### PREPARATION OF $A\beta_{25-35}$ FRAGMENT

The $A\beta_{25-35}$ fragment was prepared as described previously [Giovannelli et al., 1998]. In brief, 1 mg $A\beta_{25-35}$ was dissolved in 200, 400, or 2,000 μl sterile distilled water, for final concentrations of 5, 2.5, and 0.5 μg/μl, respectively. The samples were incubated at 37°C for 7 days to allow for fragment aggregation.

### TREATMENT PROTOCOL

Rats were housed for 7 days before experiments and were then randomly assigned to one of six groups (n = 15 per group). Rats were anesthetized by intraperitoneal injection of chloral hydrate (10%; 0.3 ml/100 g), placed in a stereotaxic instrument, the skull was opened, and the hippocampal CA1 area was positioned with respect to bregma (ML ± 2.0 mm; AP −3.5 mm; DV 2.7 mm). A microsyringe was used to inject 2 μl of solution on each side. The injection was completed within 10 min, and the needle was left in place for 5 min. Each rat in the high-, medium- and low-dose groups received a bilateral injection of 10, 5, and 1 μg $A\beta_{25-35}$ on each side, respectively. The dose of $A\beta_{25-35}$ that we used was based on previous studies [Li et al., 2005; Yao et al., 2005]. Rats in the normal saline group received injection of an equal volume of normal saline, and the sham-operation group received no injection. The normal control group received no treatment. The rats were placed into individual cages until they regained full consciousness and were maintained routinely. On days 7, 14, and 21 after operation, five rats in each group were decapitated, and hippocampal tissues were harvested and used for assays.

### TRANSMISSION ELECTRON MICROSCOPY

Hippocampal tissues were cut into 1-$mm^3$ blocks, fixed in 4% glutaraldehyde for 48 h, and postfixed in 1% osmium tetroxide for 1 h. The blocks were then dehydrated in an ethanol series, and slices were cut with an ultrathin microtome. The slices were observed under a JEM-2010 transmission electron microscope (JEOL Ltd, Tokyo, Japan).

### $CA^{2+}$-ATPASE ASSAY

$Ca^{2+}$-ATPase activity was measured with the phosphorus method, according to the manufacturer's instructions. Five rats in each group were killed at 7, 14, and 21 days after operation. Brains were removed, and the hippocampus was harvested. Approximately 0.2 g hippocampal tissue was collected from the same position of the right hippocampus from each rat and homogenized.

### PREPARATION OF ENRICHED HIPPOCAMPAL NEURONS

Trypan-blue exclusion was performed with 2% trypan blue; the percentage of viable cells was required to be greater than 95%. The isolation of hippocampal neurons was performed according to Brewer [1997], with modifications. Approximately 0.5 g of freshly harvested hippocampal tissue was shredded with a sterile razor blade. Samples were rinsed repeatedly with calcium-free Hank balanced salt solution, centrifuged at 1,000 rpm for 5 min, the

supernatant was discarded, and the precipitate was passed over a 200-μm filter. A volume of 2 ml D-Hank solution was added to the filtrate, and the samples were mixed well. The samples were then centrifuged three times at 500 rpm for 5 min; supernatant was discarded after each centrifugation. Enriched hippocampal neurons were collected and resuspended in D-Hank solution, and the cell concentration was adjusted to $10^6$ cells/ml.

### DETERMINATION OF $[CA^{2+}]_I$

Determination of $[Ca^{2+}]_i$ was performed as described previously [Asada et al., 1999]. In brief, Fluo-3/AM was dissolved in dimethylsulfoxide (DMSO), diluted to a final concentration of 1 mM in storage buffer (Fluo-3/AM dissolved in DMSO), and stored at −20°C in the dark. A volume of 10 μl Fluo-3/AM in storage buffer was added to 1 ml of the above-mentioned cell suspension (final concentration 10 μM). The samples were placed in a 37°C incubator with 5% carbon dioxide for 1 h, with light shaking three times during that period. The Fluo-3/AM-loaded cell suspension was collected and centrifuged at 1,000 rpm for 5 min. Excess dye was removed in the supernatant, and the cell pellets were rinsed with D-Hank solution three times and diluted to a final volume of 1 ml with D-Hank solution. The samples were then examined by flow cytometry (Cell Lab Quanta SC, Beckman Coulter, Brea, CA). The mean fluorescence intensity of 10,000 neurons was measured for each specimen at an excitation wavelength of 488 nm and an emission wavelength of 526 nm.

### DETERMINATION OF MITOCHONDRIAL MEMBRANE POTENTIAL

The mitochondrial membrane potential was measured as described previously [Ferlini and Scambia, 2007]. In brief, Rhodamine 123 was dissolved in DMSO, diluted to a final concentration of 5 μg/L in storage buffer (Rhodamine123 dissolved with DMSO), and stored at −20°C in the dark. A volume of 5 μl Rhodamine 123 in storage buffer was added to 1 ml of the above-mentioned cell suspension (final concentration 5 μg/ml), and the sample was mixed well. Samples were placed in an 37°C incubator with 5% carbon dioxide for 30 min. Rhodamine 123-loaded cell suspensions were then collected and centrifuged at 1,000 rpm for 5 min. Excess dye was removed by rinsing the samples with D-Hank solution three times, and the cell pellets were diluted to a final volume of 1 ml with D-Hank solution. Samples were examined by flow cytometry as above. The mean fluorescence intensity of 10,000 neurons was measured for each specimen at an excitation wavelength of 505 nm and an emission wavelength of 534 nm.

### REVERSE-TRANSCRIPTION POLYMERASE CHAIN REACTION

For RT-PCR, cDNA sequences of target genes were retrieved from the NCBI genomic library, and Primer 5.0 software (Promega Corp.) was used to design primers. Primers were synthesized by Invitrogen and are as follows: β-actin, forward 5′ GTA AAG ACC TCT ATG CCA ACA 3′, reverse 5′ GGA CTC ATC GTA CTC CTG CT 3′ (227 bp); ANT, forward 5′ CCT TGG TGA CTG CCT GGT T 3′, reverse 5′ GCC TTG CCT CCT TCG TCT 3′ (339 bp); VDAC1, forward 5′ TGA TGG GAC GGA GTT TGG 3′, reverse 5′ ACC CGC ATT GAC GTT CTT 3′ (259 bp); Cyp-D, forward 5′ GAA ATG GAC CCT TCA AAC AC 3′, reverse 5′ GCA TAC ACT GCC TTC TCT TTF 3′ (197 bp). Total RNA from rat hippocampus was extracted with a Trizol kit (Invitrogen) according to the manufacturer's instructions and quantified with an ultraviolet spectrophotometer. Extracted total RNA was used as template, and oligo DTs were used as primers for cDNA synthesis in the presence of avian myeloblastosis virus reverse transcriptase. The reaction was carried out at room temperature for 10 min, after which the samples were placed in a 42°C constant-temperature water bath for 1 h and then cooled in an ice bath for 2 min. The 25-μl reaction system contained 2.5 μl template, 2 μl 10× *Ex Taq* buffer ($Mg^{2+}$), 2 μl 2.5 mM dNTP mixture, upstream and downstream primers (0.8 μl each), and 0.35 μl *Taq* enzyme (5 U/μl). After predenaturation at 4°C for 4 min, cDNA was amplified by 30 cycles of denaturation at 94°C for 45 s, annealing at 72°C for 45 s, and extension at 72°C for 10 min. Annealing temperature for *β-actin*, *ANT*, *VDAC1*, and *Cyp-D* was 48, 46, 43.5, and 44.6°C, respectively. The PCR products were collected and separated by 2% agarose gel electrophoresis and stained with ethidium bromide. Target bands were scanned by densitometry and analyzed with a gel image analysis system (Bio-Pro 200E; Sim International Group Co. Ltd, Newark, DE).

### WESTERN BLOT

For Western blots, approximately 0.5 g of hippocampal tissue from rats in each group was collected, and total protein was extracted according to conventional methods, cooled, and stored in −80°C until use. Proteins were separated by 10% sodium dodecyl polyacrylamide gel electrophoresis at 70 V for the stacking gel and 110 V for the separation gel at 4°C for approximately 1 h and transferred to nitrocellulose membranes at 30 V and 4°C for 12 h. The membranes were rinsed and incubated with ANT goat polyclonal antibody (diluted 1:200), VDAC1 goat polyclonal antibody (diluted 1:200), Cyp-D rabbit polyclonal antibody (diluted 1:200), or β-actin rabbit polyclonal antibody (diluted 1:500) at 37°C for 2 h. After a wash, membranes were incubated with alkaline phosphatase-conjugated anti-rabbit secondary antibody (1:3,500) or alkaline phosphatase-conjugated anti-goat secondary antibody for 30 min, washed, and chromogenic reagent was added for color development. Developed bands were scanned and analyzed by densitometry.

Values for all measurements are expressed as the mean ± SD. Statistical analysis was performed using ANOVA, followed by two by two comparisons adjusted by Bonferroni approach. Data were analyzed using SAS 9.0 (SAS Institute, Inc., Cary, NC). All *P* values were two-sided and were considered significant if *P* was less than 0.05.

## RESULTS

Transmission electron microscopy was performed for each experimental group at 7, 14, and 21 days after intrahippocampal injection of $A\beta_{25-35}$. Hippocampal structure in the sham-operation group (Fig. 1A) was not significantly different from that in the normal control group (Fig. 1B) at 21 days after injection; the neurons were intact, and the mitochondrial number and appearance of mitochondrial organelles was normal. At days 7 and 14, slight changes were observed in the mitochondria (data not shown). At 21 days, necrotic neurons were apparent in the high-dose group (10 μg/rat), and

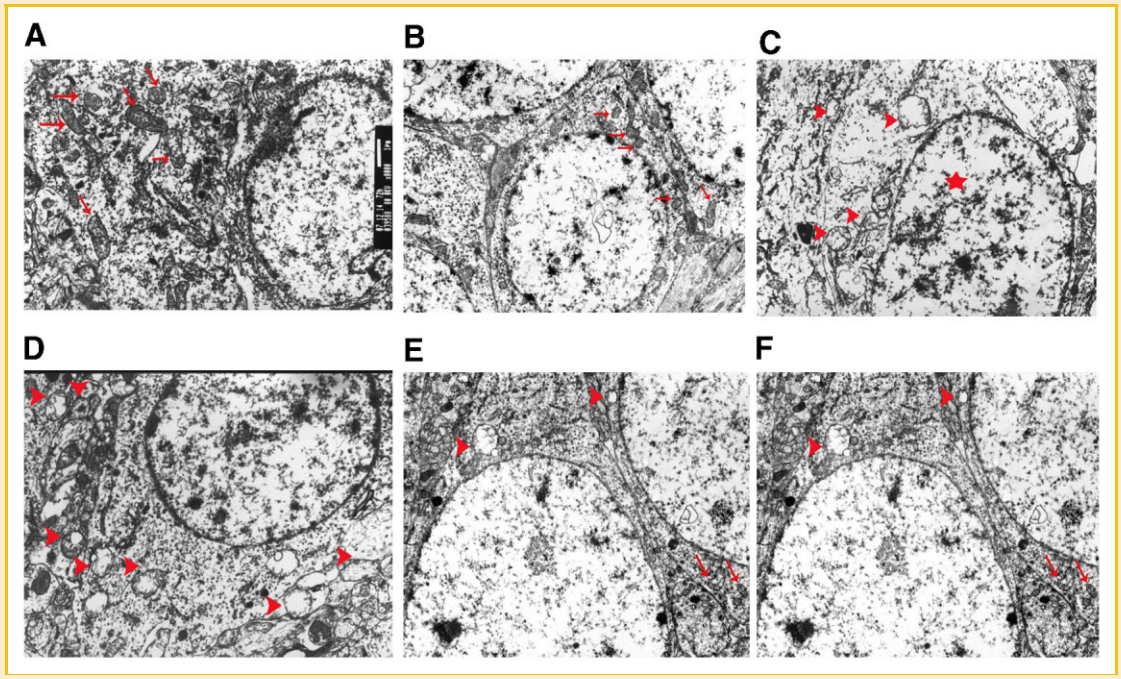


Fig. 1. Representative transmission electron microscopy images of hippocampal tissue from rats subjected to intrahippocampal injection of amyloid $A\beta_{25-35}$ fragment at 21 days after injection. Ninety rats were assigned to one of six groups (n = 15 group): (A) Sham-operation group, (B) normal control group, (C) high-dose group (10 μg/rat), (D) medium-dose group (5 μg/rat), (E) low-dose group (1 μg/rat), (F) saline group. Arrows indicate normal mitochondria, arrowheads indicate abnormal swelling of mitochondria, and star indicates a pyknotic nucleus. Magnification 5,000×. [Color figure can be viewed in the online issue, which is available at wileyonlinelibrary.com.]

nuclear pyknosis, partial nuclear membrane dissolution and disappearance, and mitochondrial deformation, swelling, and reduction in number was observed (Fig. 1C). The typical inner membrane cristae of mitochondria could still be seen in some swollen bodies, indicating that these swollen bodies represented damaged mitochondria. In the medium-dose group (5 μg/rat) at 21 days, some of the mitochondria had degenerated, and vacuolar degeneration was obvious (Fig. 1D). In the low-dose group (1 μg/rat) at 21 days, a small number of mitochondria had degenerated (Fig. 1E). Mitochondrial degeneration was observed in very few cells in the saline group (Fig. 1F).Repeated measures analysis of variance and group mean comparisons showed that hippocampal $Ca^{2+}$-ATPase activity in rats injected with 1, 5, or 10 μg $A\beta_{25-35}$ was significantly ($P < 0.01$) lower than that in the saline group at each time point (with the exception of the 1 μg group at 14 days), showing a clear dose–response relation (Fig. 2A). There were no significant differences among the sham-operation, saline, and normal control groups.

The $Ca^{2+}$-specific fluorescent probe, Fluo-3/AM was used to assess $[Ca^{2+}]_i$ in isolated hippocampal neurons. Mean fluorescence intensity of 10,000 neurons in each group was detected by flow cytometry. Repeated measures analysis of variance and group mean comparisons showed that $[Ca^{2+}]_i$ increased with dose and time in groups injected with 5 or 10 μg $A\beta_{25-35}$ compared with the saline group (Fig. 2B). The 5-μg group reached significance ($P < 0.01$) at 21 days, whereas the 10-μg group did so at 14 and 21 days. There were no significant differences in $[Ca^{2+}]_i$ among the sham-operation, saline, and normal control groups.

Rhodamine123 was used to measure changes in mitochondrial membrane potential in 10,000 hippocampal neurons at different time points. Repeated measures analysis of variance and group mean comparisons showed that intracellular mitochondrial membrane potential in rats injected with 1, 5, or 10 μg $A\beta_{25-35}$ decreased significantly ($P < 0.05$) with dose and time compared with the saline group, showing clear time- and dose-response relations (Fig. 2C). There were no significant differences in intracellular mitochondrial membrane potential among the sham-operation, saline, and normal control groups.

We then investigated whether the $A\beta_{25-35}$-induced decrease in intracellular mitochondrial membrane potential was associated with the expression of genes associated with the MPTP. We used RT-PCR to detect the expression of genes associated with the MPTP including *VDAC*, *ANT*, and *Cyp-D*. Results showed that expression levels of *VDAC*, *ANT*, and *Cyp-D* genes (normalized to *β-actin* expression) in the 1, 5, and 10 μg groups were significantly ($P < 0.05$) higher than those in the normal saline group at each time point (Fig. 3A–C). There were no significant differences among the sham-operation, saline, and normal control groups.

Western blot results showed that the expression levels of proteins associated with the MPTP (normalized to β-actin expression) in the 1, 5, and 10 μg groups were all significantly ($P < 0.05$) increased compared to the normal saline group at each time point (Fig. 4A–D). There were no significant differences among the sham-operation, saline, and normal control groups.

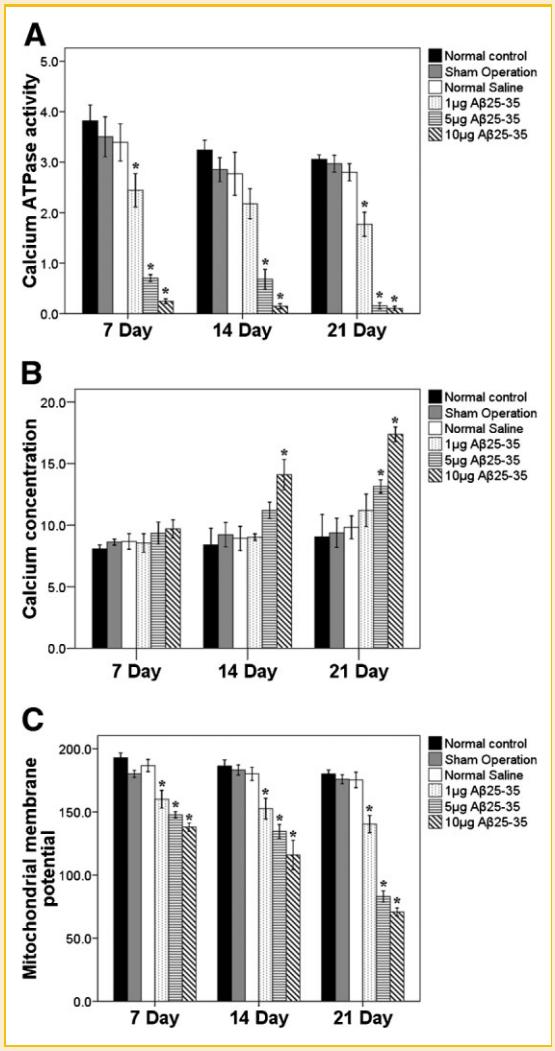


Fig. 2. A: $Ca^{2+}$-ATPase activity in rat hippocampal tissue measured at 7, 14, and 21 days after injection of 1, 5, or 10 μg amyloid $A\beta_{25-35}$ fragment (or controls) (n = 5 rats per group). Data are shown as mean ± standard deviation (SD). $^{*}P < 0.01$ versus normal saline group. B: Measurement of $[Ca^{2+}]_i$ in rat hippocampal neurons measured at 7, 14, and 21 days after injection of 1, 5, or 10 μg amyloid $A\beta_{25-35}$ fragment (or controls) (n = 5 rats per group). Fluo-3/AM fluorescence of 10,000 neurons in each group was assessed by flow cytometry. Data are shown as mean ± standard deviation (SD). $^{*}P < 0.01$ versus normal saline group. C: Measurement of mitochondrial membrane potential in rat hippocampal neurons at 7, 14, and 21 days after injection of 1, 5, or 10 μg amyloid $A\beta_{25-35}$ fragment (or controls) (n = 5 rats per group). Rhodamine 123 fluorescence of 10,000 neurons in each group was assessed by flow cytometry. Data are shown as mean ± standard deviation (SD). $^{*}P < 0.05$ versus normal saline group.

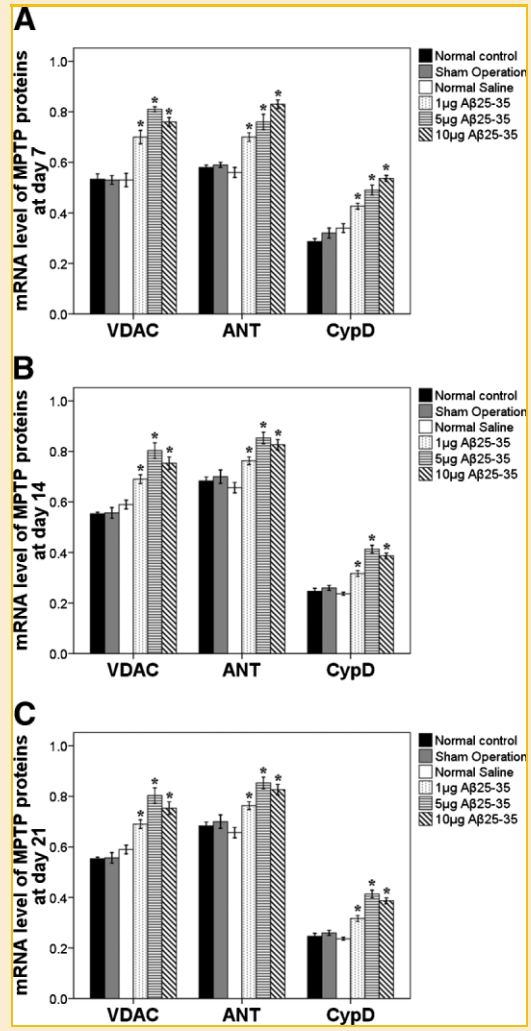


Fig. 3. Determination of expression of genes associated with the MPTP by reverse-transcription polymerase chain reaction in rat hippocampal neurons at 7, 14, and 21 days after injection of 1, 5, or 10 μg amyloid $A\beta_{25-35}$ fragment (or controls) (n = 5 rats per group). A: day 7 after injection. B: day 14 after injection. C: day 21 after injection. Data are shown as mean ± standard deviation (SD). $^{*}P < 0.05$ versus normal saline group. VDAC, voltage-dependent anion channel; ANT, adenine nucleotide translocator; Cyp-D, cyclophilin D.

## DISCUSSION

The aim of the present study was to evaluate the effect of β-amyloid fragment $A\beta_{25-35}$ on mitochondrial structure and function and the expression of genes associated with the MPTP in rat hippocampal neurons. Transmission electron microscopy of hippocampal tissue from rats injected with $A\beta_{25-35}$ showed structural damage of neurons and apoptotic-like changes and, in particular, changes in mitochondrial structure and quantity, reflective of mitochondrial dysfunction. Flow cytometric results of enriched hippocampal neurons showed significantly decreased $Ca^{2+}$-ATPase activity, significantly increased $[Ca^{2+}]_i$, and significantly decreased mitochondrial membrane potential in response to $A\beta_{25-35}$ injection compared to the saline control group, further reflecting damage. The significance of these alterations was variably dose and time dependent.

We also assessed MPTP-related gene and protein expression by RT-PCR and Western blot. To our knowledge, this has not been reported in relation to $A\beta_{25-35}$ treatment in rat hippocampal tissue. All dose groups (1, 5, and 10 μg) showed statistically significant

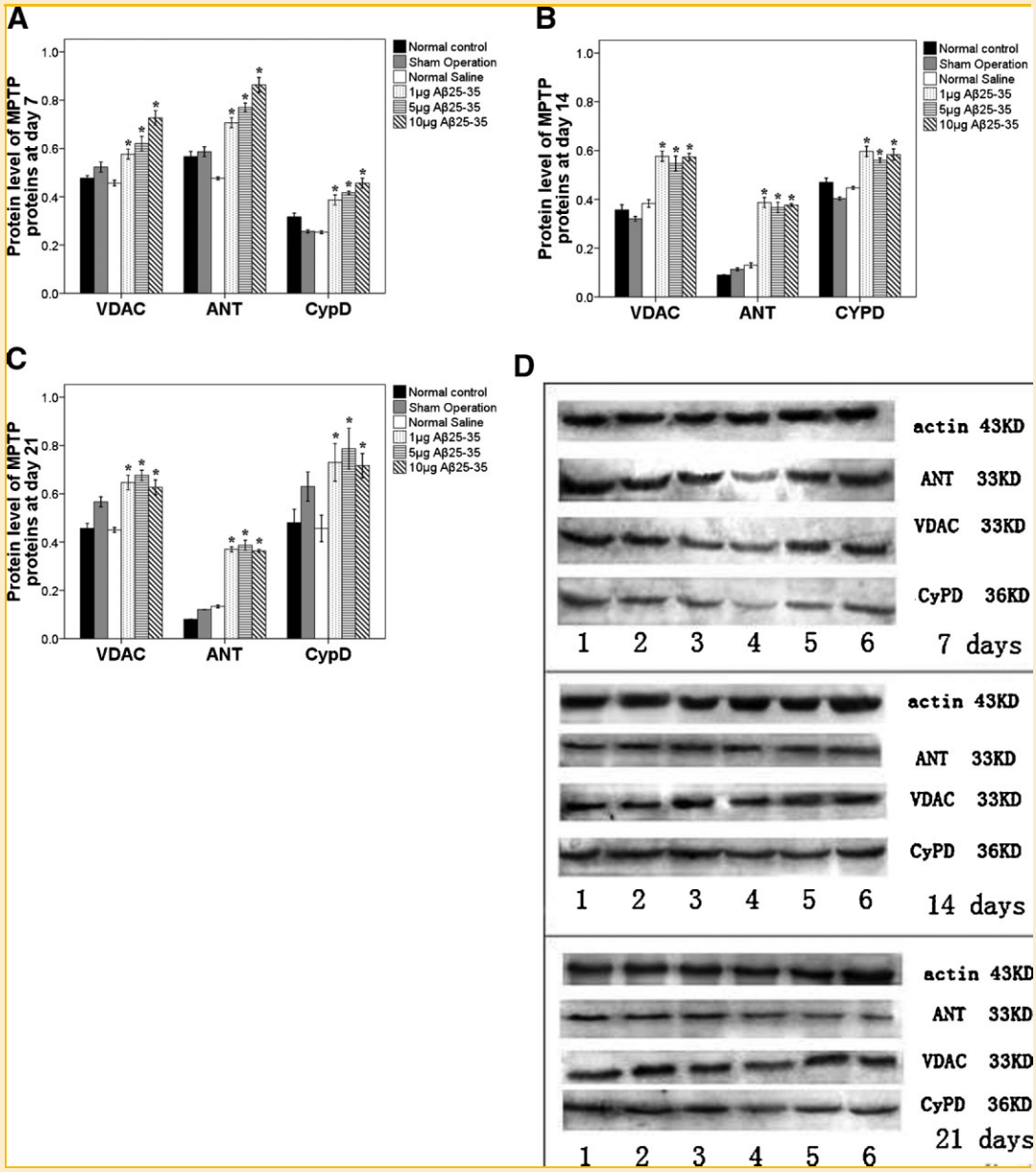


Fig. 4. Determination of expression of proteins associated with the MPTP by Western blot in rat hippocampal neurons at 7, 14, and 21 days after injection of 1, 5, or 10 μg amyloid $A\beta_{25-35}$ fragment (or controls) ($n = 5$ rats per group). A: day 7 after injection. B: day 14 after injection. C: day 21 after injection. D: Representative Western blot results. Lane 1, 10 μg $A\beta_{25-35}$ group; lane 2, 5 μg $A\beta_{25-35}$ group; lane 3, 1 μg $A\beta_{25-35}$ group; lane 4, sham-operation group; lane 5, saline group; lane 6, normal control group. Data are shown as mean ± standard deviation (SD). $^*P < 0.05$ versus normal saline group. VDAC, voltage-dependent anion channel; ANT, adenine nucleotide translocator; Cyp-D, cyclophilin D.

increases in mRNA and protein for *VDAC*, *ANT*, and *Cyp-D* compared to the control group at 7, 14, and 21 days after injection. With the exception of *VDAC* mRNA, the effects appeared to be dose-dependent at the earliest time point (7 days after injection), after which the effects were similar. A recent study has also reported changes in mitochondrial gene expression in response to treatment with Aβ peptide [Manczak et al., 2010]. Specifically, cultured mouse N2a neuroblastoma cells showed increased expression of mitochondrial fission genes and decreased expression of fusion genes and peroxiredoxins.

One possible explanation for the present effect of $A\beta_{25-35}$ injection involves the inhibition of $Ca^{2+}$-ATPase activity in the neuronal plasma membrane, overexpression of proteins associated with the MPTP, and opening of the MPTP, thereby collapsing the mitochondrial membrane potential [Moreira et al., 2001], disrupting oxidative phosphorylation, and decreasing ATP generation. Cellular energy depletion may then become aggravated, potentially resulting in the initiation of apoptosis [Reddy, 2009; Du and Yan, 2010]. Another possibility is that the increased expression of proteins associated with the MPTP may be a result of an increased turnover

of these proteins, owing to oxidative damage resulting from mitochondrial dysfunction. A study by Du et al. [2008] reported that Cyp-D-deficient mice showed attenuated mitochondrial and neuronal alterations in response to Aβ treatment. Our present results may indicate that increased Cyp-D expression aggravates the effects of Aβ. Aβ binds to Cyp-D and potentially also to ANT [Du et al., 2008; Singh et al., 2009], which may increase MPTP opening. With the exception of $[Ca^{2+}]_i$ at 7 days, $A\beta_{25-35}$ injection resulted in changes in all parameters assayed at each time point. Therefore, whether the increased expression of proteins associated with the MPTP occurs in response to the $Ca^{2+}$-associated alterations and changes in mitochondrial membrane potential or precedes these changes is unclear. A more detailed examination of the time dependence of the effects may shed light on this issue.A potential limitation of the present study that we assessed the effects of the $A\beta_{25-35}$ fragment and not the reverse ($A\beta_{35-25}$) or other Aβ forms; therefore, the specificity of the $A\beta_{25-35}$ fragment was not determined. However, we did include normal saline injection and sham-operation groups to control for ionic and injection effects. In addition, the transmission electron microscopy results were described qualitatively. A quantitative approach may have provided statistically analyzable data. We did not determine neuron purity in the cell suspensions used for $Ca^{2+}$ and membrane potential assays. The method used results in an enrichment of hippocampal neurons. However, some glial cells were likely present.In conclusion, we report $A\beta_{25-35}$-induced increases in the expression of genes and proteins associated with the MPTP in rat hippocampal neurons. In addition to the effects on mitochondrial structure and function, these results may aid in elucidating the mechanism of Aβ accumulation and neurodegeneration in diseases such as Alzheimer disease.

## ACKNOWLEDGMENTS

This study was funded by the Chinese National Natural Science Foundation (30600504). We would like to thank the professors and students of the Department of Health and Toxicology, School of Public Health, Harbin Medical University, for their help and support. We also appreciate the help and support of Mr. Yanhui Gao and Ms. Lin Gao of the Key Laboratory of Epidemiology and Etiology, Ministry of Health, Endemic Disease Prevention and Treatment Center, Chinese Disease Control Center.

## REFERENCES

Abramov AY, Canevari L, Duchen MR. 2004. Beta-amyloid peptides induce mitochondrial dysfunction and oxidative stress in astrocytes and death of neurons through activation of NADPH oxidase. J Neurosci 24:565–575.

Asada Y, Yamazawa T, Hirose K, Takasaka T, Iino M. 1999. Dynamic Ca2+ signalling in rat arterial smooth muscle cells under the control of local renin-angiotensin system. J Physiol 521:497–505.

Baumgartner HK, Gerasimenko JV, Thorne C, Ferdek P, Pozzan T, Tepikin AV, Petersen OH, Sutton R, Watson AJ, Gerasimenko OV. 2009. Calcium elevation in mitochondria is the main $Ca^{2+}$ requirement for mitochondrial permeability transition pore (mPTP) opening. J Biol Chem 284:20796–20803.

Brewer GJ. 1997. Isolation and culture of adult rat hippocampal neurons. J Neurosci Meth 71:143–155.

Burchell VS, Gandhi S, Deas E, Wood NW, Abramov AY, Plun-Favreau H. 2010. Targeting mitochondrial dysfunction in neurodegenerative disease: Part II. Expert Opin Ther Targets 14:497–511.

Casley CS, Land JM, Sharpe MA, Clark JB, Duchen MR, Canevari L. 2002. Beta-amyloid fragment25-35 causes mitochondrial dysfunction in primary cortical neurons. Neurobiol Dis 10:258–267.

Celsi F, Pizzo P, Brini M, Leo S, Fotino C, Pinton P, Rizzuto R. 2009. Mitochondria, calcium and cell death: A deadly triad in neurodegeneration. Biochim Biophys Acta 1787:335–344.

Chen JX, Yan SD. 2007. Amyloid-beta-induced mitochondrial dysfunction. J Alzheimers Dis 12:177–184.

Du H, Yan SS. 2010. Mitochondrial permeability transition pore in Alzheimer's disease: Cyclophilin D and amyloid beta. Biochim Biophys Acta 1802:198–204.

Du H, Guo L, Fang F, Chen D, Sosunov AA, McKhann GM, Yan Y, Wang C, Zhang H, Molkentin JD, Gunn-Moore FJ, Vonsattel JP, Arancio O, Chen JX, Yan SD. 2008. Cyclophilin D deficiency attenuates mitochondrial and neuronal perturbation and ameliorates learning and memory in Alzheimer's disease. Nat Med 14:1097–1105.

Emerit J, Edeas M, Bricaire F. 2004. Neurodegenerative diseases and oxidative stress. Biomed Pharmacother 58:39–46.

Ferlini C, Scambia G. 2007. Assay for apoptosis using the mitochondrial probes, Rhodamine123 and 10-N-nonyl acridine orange. Nat Protoc 2:3111–3114.

Ferreiro E, Oliveira CR, Pereira CM. 2008. The release of calcium from the endoplasmic reticulum induced by amyloid-beta and prion peptides activates the mitochondrial apoptotic pathway. Neurobiol Dis 30:331–342.

Galiegue S, Tinel N, Casellas P. 2003. The peripheral benzodiazepine receptor: A promising therapeutic drug target. Curr Med Chem 10:1563–1572.

Giovannelli L, Scali C, Faussone-Pellegrini MS, Pepeu G, Casamenti F. 1998. Long-term changes in the aggregation state and toxic effects of beta-amyloid injected into the rat brain. Neuroscience 87:349–357.

Halestrap AP. 2009. What is the mitochondrial permeability transition pore? J Mol Cell Cardiol 46:821–831.

Halestrap AP, Clarke SJ, Javadov SA. 2004. Mitochondrial permeability transition pore opening during myocardial reperfusion—A target for cardioprotection. Cardiovasc Res 61:372–385.

Kroemer G. 2003. The mitochondrial permeability transition pore complex as a pharmacological target. An introduction. Curr Med Chem 10:1469–1472.

Li F, Li GR, Man YQ. 2005. The difference of spatial memory in rats induced by β-Amyloid 25–35 injection. Pharm Biotechnol 12:190–192.

Manczak M, Mao P, Calkins MJ, Cornea A, Reddy AP, Murphy MP, Szeto HH, Park B, Reddy PH. 2010. Mitochondria-targeted antioxidants protect against amyloid-beta toxicity in Alzheimer's disease neurons. J Alzheimers Dis 20:S609–S631.

Mark RJ, Hensley K, Butterfield DA, Mattson MP. 1995. Amyloid beta-peptide impairs ion-motive ATPase activities: Evidence for a role in loss of neuronal Ca2+ homeostasis and cell death. J Neurosci 15:6239–6249.

Millucci L, Ghezzi L, Bernardini G, Santucci A. 2010. Conformations and biological activities of amyloid beta peptide 25–35. Curr Protein Pept Sci 11:54–67.

Moreira PI, Santos MS, Moreno A, Oliveira C. 2001. Amyloid beta-peptide promotes permeability transition pore in brain mitochondria. Biosci Rep 21:789–800.

Muirhead KE, Borger E, Aitken L, Conway SJ, Gunn-Moore FJ. 2010. The consequences of mitochondrial amyloid beta-peptide in Alzheimer's disease. Biochem J 426:255–270.

Reddy PH. 2009. Amyloid beta, mitochondrial structural and functional dynamics in Alzheimer's disease. Exp Neurol 218:286–292.

Singh P, Suman S, Chandna S, Das TK. 2009. Possible role of amyloid-beta, adenine nucleotide translocase and cyclophilin-D interaction in mitochondrial dysfunction of Alzheimer's disease. Bioinformation 3:440–445.

Yao CB, Yuan H, Zhao JJ. 2005. Expression of HSP70 in hippocampus neurons of Alzheimer's model rats induced by Aβ25–35. Chin J Gerontol 6:680–682.

Zhu D, Lai Y, Shelat PB, Hu C, Sun GY, Lee JC. 2006. Phospholipases A2 mediate amyloid-beta peptide-induced mitochondrial dysfunction. J Neurosci 26:11111–11119.

Zorov DB, Juhaszova M, Yaniv Y, Nuss HB, Wang S, Sollott SJ. 2009. Regulation and pharmacology of the mitochondrial permeability transition pore. Cardiovasc Res 83:213–225.